DALTON
FULL PAPER

Unprecedented pseudo-trigonal-bipyramidal intermediate-spin iron(III) complex: synthesis, crystal structure and magnetic properties of [Fe(4,4′-bipy)$_2$(NCS)$_3$]·(CH$_3$)$_2$CO

Nicolás Moliner,[a] José Antonio Real,*[a] M. Carmen Muñoz,[b] Ramón Martínez-Mañez[c] and Juan Modesto Clemente Juan[a]

[a] *Departament de Química Inorgànica, Universitat de València, Dr. Moliner 50, 46100, Burjassot (València), Spain*
[b] *Departamento de Física Aplicada, Universidad Politecnica de Valencia, Camino de Vera s/n, 46071, Valencia, Spain*
[c] *Departamento de Química, Universidad Politecnica de Valencia, Camino de Vera s/n, 46071, Valencia, Spain*

Received 2nd December 1998, Accepted 16th February 1999

The intermediate-spin five-co-ordinate complex [Fe(4,4′-bipy)$_2$(NCS)$_3$]·(CH$_3$)$_2$CO has been prepared, its structure determined and magnetic properties characterized. The structure is made up of mononuclear neutral species linked by van der Waals interactions. The co-ordination polyhedron is defined by five nitrogen atoms around the iron(III) ion in a distorted trigonal bipyramid. The three vertices of the equatorial plane are occupied by the thiocyanate ligands while the 4,4′-bipyridine ligands fill the axial positions. The Fe–N(CS) distances are 2.025(7), 2.04(2) and 2.02(2) Å and the axial Fe–N bond distances are 2.28(2) and 2.21(2) Å. The magnetic properties are consistent with an $S = 3/2$ ground state. The zero-field splitting in the ground state was found to be *ca.* 6 cm^{-1}. Variable temperature EPR spectra are briefly reported.

The magnetic properties of mononuclear iron(III) complexes are generally well understood. Iron(III) has the 3d^5 outer electronic configuration and hence its octahedral complexes may be either high spin ($S = 5/2$) (HS) or low spin ($S = 1/2$) (LS). The HS ground configuration is adopted when relatively weak-field ligands are co-ordinated while the LS electronic configuration is adopted when strong-field ligands are involved. The majority of iron(III) compounds can be classified in one of these two types. Furthermore, a relatively small number of six-co-ordinate iron(III) compounds can adopt the two electronic configurations. A thermal LS to HS spin transition occurs for this kind of compounds, so-called spin-crossover compounds.

Iron(III) can also exhibit an intermediate spin (IS) ($S = 3/2$) state. The existence of this state has been either ignored for many years or specifically excluded by ligand field theory for octahedral and tetrahedral complexes.[1] Examples of iron(III) complexes with IS ground state are scarce although their existence is now well documented. In this regard, the family of bis(dialkyldithiocarbamato)halogenoiron(III) complexes is paradigmatic, since it was the first systematically studied.[2] Nevertheless, most of the IS and the related spin-admixed iron(III) compounds belong to the co-ordination chemistry of tetraamido and tetraazamacrocyclic ligands,[3,4] porphyrins,[5–9] and phthalocyanines.[10–12] The occurrence of highly distorted geometries is the common structural feature of these systems. Distorted square-pyramidal geometry is by far the most observed. In such a geometry the axial ligand field is very weak compared to the equatorial one, so the $d_{x^2-y^2}$ atomic orbital lies well above the d_{z^2} in energy and remains unoccupied. Hence, the $S = 3/2$ becomes the ground state.

Trigonal bipyramidal geometry is uncommon in the co-ordination chemistry of iron(III).[13] As far as we are aware, no example of an $S = 3/2$ spin ground state in this geometry has been reported up to now. In this context, the present contribution deals with the characterization of [Fe(4,4′-bipy)$_2$(NCS)$_3$]·(CH$_3$)$_2$CO **1** which constitutes the first example of a pseudo-trigonal bipyramidal intermediate-spin iron(III) complex.

Experimental

Materials

Iron(II) sulfate heptahydrate, 4,4′-bipyridine (4,4′-bipy) and potassium thiocyanate were purchased from commercial sources and used as received. Elemental analyses (C, H, N) were performed by the Microanalytical Service of the Universidad Autónoma de Madrid (Spain). All the manipulations were carried out under an argon atmosphere except for the final evaporation where the solution was allowed to concentrate under atmospheric conditions.

Preparation of [Fe(4,4′-bipy)$_2$(NCS)$_3$]·(CH$_3$)$_2$CO 1

To a solution of KNCS (0.5 mmol) in acetone (10 cm^3) was added 0.25 mmol of FeSO$_4$·7H$_2$O. The mixture was stirred at room temperature for 20 min, decanted off, and filtered. The resulting 1 : 2 Fe^{II} : NCS$^-$ red solution was added dropwise to an acetone solution of 4,4′-bipy (0.5 mmol, 40 cm^3). An orange-red precipitate of [Fe(4,4′-bipy)(H$_2$O)$_2$]·4,4′-bipy was formed immediately. It was separated by filtration. Upon slow evaporation of the filtrate well shaped violet crystals of complex **1** were obtained together with small orange-red crystals of [Fe(4,4′-bipy)(H$_2$O)$_2$]·4,4′-bipy after a week. The violet crystals were separated mechanically from different syntheses and used for X-ray diffraction and magnetic measurements. Yield *ca.* 4% (Found: C, 51.4; H, 3.5; N, 16.4. Calc. for C$_{26}$H$_{22}$FeN$_7$OS$_3$: C, 52.00; H, 3.66; N, 16.32%).

Physical techniques

The variable temperature magnetic susceptibility measurements

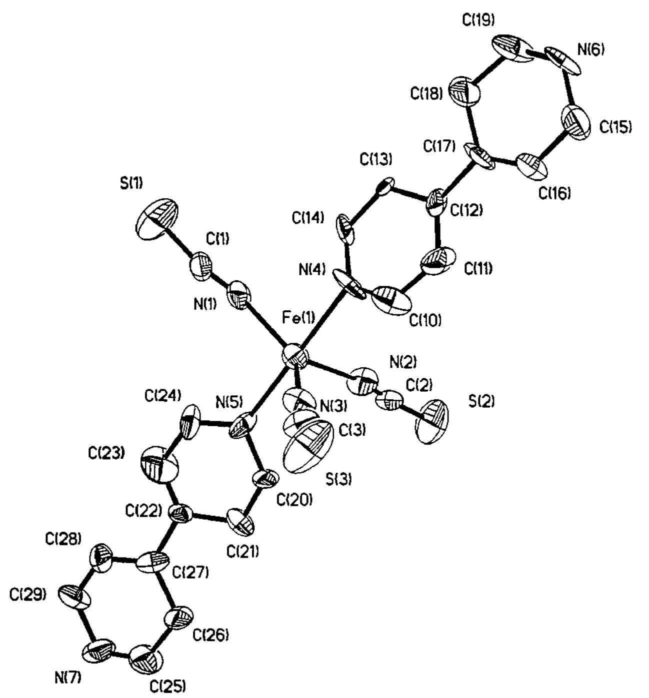

Fig. 1 Perspective drawing of complex **1** with the atom numbering scheme (50% probability displacement ellipsoids).

were carried out on a microcrystalline sample (4 mg) using a Quantum Design MPMS2 SQUID susceptometer equipped with a 55 kG magnet and operating at 10 kG in the range of 1.8–400 K. The susceptometer was calibrated with $[NH_4]_2Mn[SO_4]_2\cdot 12H_2O$. The correction for diamagnetism was estimated from Pascal constants as -313×10^{-6} cm³ mol⁻¹.

The EPR spectrum was recorded on a powdered sample at X-band frequency with a Bruker ER200D spectrometer equipped with an Oxford Instruments continuous-flow cryostat working in the 4.2–300 K temperature range.

Crystallographic data collection and structure determination

Diffraction data on a prismatic crystal of dimensions 0.1 × 0.1 × 0.05 mm were collected at 293 K with a Siemens P-4 diffractometer using graphite-monochromated Mo-Kα radiation ($\lambda = 0.71073$ Å) and the θ–2θ scan technique. The cell parameters were determined from least-squares refinement of 25 well centered reflections in the range $12 < \theta < 20$. Crystal parameters and refinement data are summarized in Table 1. Three standard reflections were monitored every hour, but no intensity variations were observed. Lorentz-polarization and absorption corrections were applied to the data. The structure was solved by direct methods using SHELXS 86 and refined by the full-matrix least-squares method on F^2 using SHELXL 93.[14] All non-hydrogen atoms were refined anisotropically. All hydrogen atoms were placed in computed positions and isotropically refined.

Selected bond distances and angles are listed in Table 2.

CCDC reference number 186/1357.

Results and discussion

Description of the structure

The crystal structure of complex **1** consists of discrete $[Fe(4,4'\text{-bipy})_2(NCS)_3]$ neutral molecular units linked by van der Waals interactions. Fig. 1 shows a view of the complex with the numbering scheme. The co-ordination polyhedron is defined by five nitrogen atoms around the iron atom in a distorted trigonal bipyramid. The equatorial plane is constituted by three nitrogen atoms [N(1), N(2) and N(3)] belonging to the thiocyanate groups while the apical positions are occupied by two nitrogen atoms [N(4) and N(5)] of two different 4,4′-bipy ligands. The iron atom lies in the equatorial plane; the observed deviation is 0.036(13) Å. The Fe–N bond lengths involving the NCS^- groups, 2.025(7), 2.04(2) and 2.02(2) Å for N(1), N(2) and N(3), are shorter than those involving the 4,4′-bipy ligands, 2.28(2) and 2.21(2) Å for N(4) and N(5), respectively.

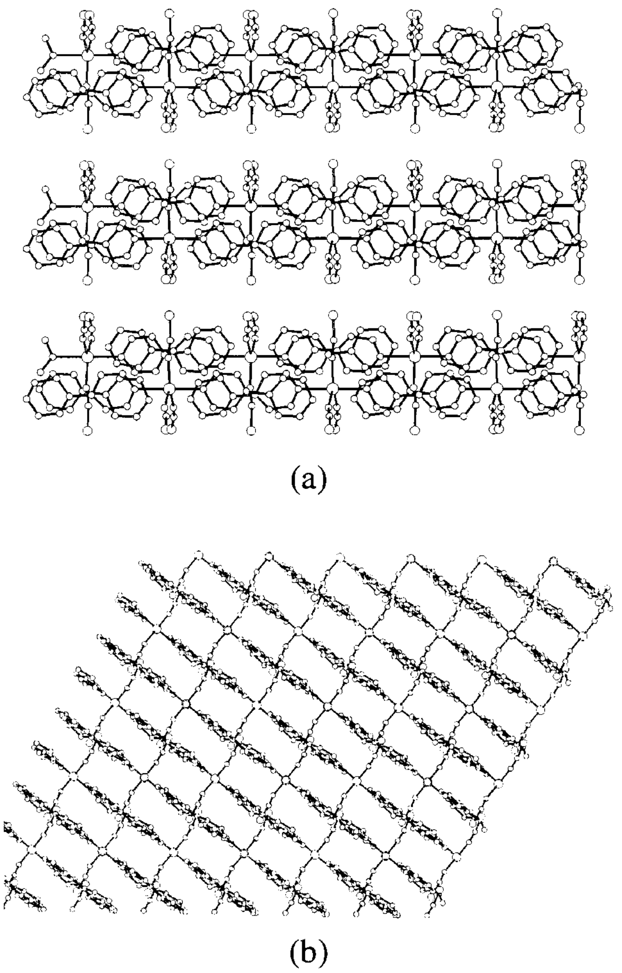

Fig. 2 (a) A view of the packing showing the stacking of the sheets along the [010] direction and the π interaction between pyridyl groups along the [100] direction. (b) View of a sheet along the [010] direction.

To the best of our knowledge there are only two structural studies of a trigonal-bipyramidal geometry for iron(III) complexes which concern the $[Fe(N_3)_5]^{2-}$ [15] and $[Fe(4\text{-CNpy})_2Cl_3]$[16] high spin molecules. The average axial iron(III)–nitrogen bond lengths for $[Fe(N_3)_5]^{2-}$ and **1** are significantly different [2.04(1) against 2.245(2) Å], whereas the corresponding equatorial iron(III)–nitrogen ones are similar [1.97(4) against 2.03(2) Å]. By contrast, the axial metal to ligand distances of **1** compare well with those of $[Fe(4\text{-CNpy})_2Cl_3]$, the average values being 2.24(2) and 2.221(3) Å respectively.

Noticeable thermal agitation in the crystal causes departure from linearity for the thiocyanate groups [N(1)–C(1)–S(1) 170(3), N(2)–C(2)–S(2) 175(2) and N(3)–C(3)–S(3) 173(2)°], typical values being in the 175–178° range.[17] The bending angles of Fe–N(1)–C(1), Fe–N(2)–C(2) and Fe–N(3)–C(3) are 170(3), 166(2) and 172(2)°, respectively. The two pyridine rings of each 4,4′-bipy ligand are not coplanar, the dihedral angles being 10.13(6) and 14.01(7)° for the 4,4′-bipy ligands defined by the N(5) and N(4) atoms, respectively. The two pyridine rings connected by the iron atom define a dihedral angle of 32.4(6)°. The distortion from the idealized D_{3h} point group symmetry mainly occurs in the three (SCN)–Fe–(NCS) angles N(1)–Fe–N(2) 124.4(9), N(1)–Fe–N(3) 128.0(10) and N(2)–Fe–N(3) 107.5(3)°,

Table 1 Crystal data and structure refinement for complex **1**

Empirical formula	$C_{26}H_{22}FeN_7OS_3$
Formula weight	600.54
Crystal system	Monoclinic
Space group	*Cc*
a/Å	14.209(5)
b/Å	19.533(6)
c/Å	12.085(4)
β/°	119.04(2)
V/Å^3, Z	2932(2), 4
D_c/Mg m^{-3}	1.360
μ/mm^{-1}	0.760
Data/restraints/parameters	2010/26/343
Goodness of fit on F^2	0.915
Final $R1$, $wR2$ [$I > 2\sigma(I)$]	0.0444, 0.1126
(all data)	0.0844, 0.1456

Table 2 Selected bond lengths (Å) and angles (°) for complex **1**

Fe(1)–N(1)	2.025(7)	Fe(1)–N(2)	2.04(2)
Fe(1)–N(3)	2.02(2)	Fe(1)–N(4)	2.28(2)
Fe(1)–N(5)	2.21(2)	S(1)–C(1)	1.627(11)
S(2)–C(2)	1.66(3)	S(3)–C(3)	1.59(3)
N(1)–C(1)	1.154(11)	N(2)–C(2)	1.11(3)
N(3)–C(3)	1.19(3)	N(4)–C(10)	1.27(3)
N(4)–C(14)	1.31(3)	N(5)–C(24)	1.32(2)
N(1)–Fe(1)–N(3)	128.0(10)	N(1)–Fe(1)–N(2)	124.4(9)
N(3)–Fe(1)–N(2)	107.5(3)	N(1)–Fe(1)–N(5)	92.1(7)
N(3)–Fe(1)–N(5)	88.9(7)	N(2)–Fe(1)–N(5)	91.7(7)
N(1)–Fe(1)–N(4)	88.5(9)	N(3)–Fe(1)–N(4)	88.3(8)
N(2)–Fe(1)–N(4)	90.6(7)	N(5)–Fe(1)–N(4)	176.8(10)
N(1)–C(1)–S(1)	170(3)	N(2)–C(2)–S(2)	175(2)
N(3)–C(3)–S(3)	173(2)		

which deviate from 120°, but also in the non-linearity of the N(4)–Fe–N(5) 176.8(10)° bond angle concerning the two 4,4′-bipy ligands.

The crystal packing may be described as an arrangement of parallel sheets stacked along the [010] direction. The acetone molecules are inserted in between the sheets. A closer packing is achieved by the overlapping of the 4,4′-bipy ligands of two neighboring complex molecules within a sheet. The shortest contacts are in the 3.5–3.6 Å range and correspond to the π stacking of the pyridine rings in the [100] direction (see Fig. 2).

Magnetic properties

The magnetic properties of complex **1** in the form of the $\chi_m T$ *versus* T plot are shown in Fig. 3. At room temperature $\chi_m T$ is equal to 2.6 cm^3 K mol^{-1}, a value which is much below that expected for an $S = 5/2$ ground state ($\chi_m T = 4.3$ cm^3 K mol^{-1}) and substantially larger than the spin-only value for an $S = 3/2$ ground state (1.87 cm^3 K mol^{-1}). However, the $\chi_m T$ value for **1** lies within the 1.87–2.8 cm^3 K mol^{-1} range observed for IS phthalocyanine and porphyrin iron(III) complexes (see for instance refs. 5, 8, 18 and 19). As the temperature is lowered, $\chi_m T$ remains constant down to *ca.* 40 K, then decreases very rapidly to $\chi_m T = 1.50$ cm^3 K mol^{-1} at 2 K. No maximum of susceptibility is observed in the temperature range explored. The sharp decrease at low temperatures is reminiscent of systems having zero-field splitting (D) of the ground state of Fe^{III} and/or very weak intermolecular magnetic interactions. The former factor should be dominant at low temperatures keeping in mind the mononuclear nature of **1** and the great intra- and inter-sheet iron–iron separations (7–11 Å).

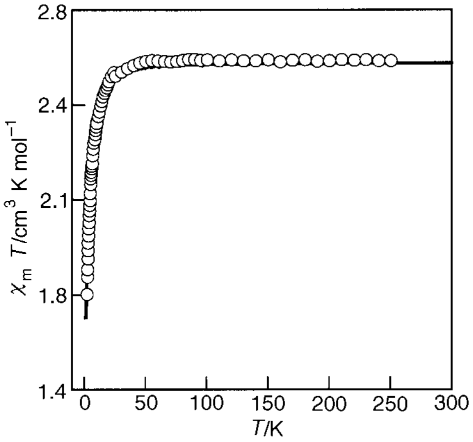

Fig. 3 Temperature variation of $\chi_m T$ for complex **1**.

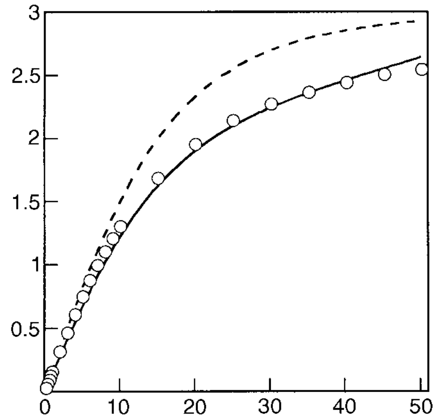

Fig. 4 Magnetization plot at 2 K for complex **1**.

We have performed magnetization measurements in order to get an estimate of D, g_z and $g_{x,y}$ parameters. The field dependence of the magnetization, $M = f(H)$, at 2 K is given in Fig. 4. The magnetization varies linearly with the field up to *ca.* 6 kG and then progressively tends to saturation. Nevertheless, it is obvious that the experimental M values are slightly less than the theoretical ones calculated with the Brillouin function for an $S = 3/2$ ground state with $g = 2$ (dashed line in Fig. 4). Magnetization measurements in the temperature range 2–20 K with applied fields of 10, 20, 30, 40 and 50 kG were performed in order better to characterize this feature [see Fig. 5(a)]. A selection of the data in the form of $M = f(H/T)$ curves is shown in Fig. 5(b). The variation of M with H/T would follow that predicted by the Brillouin function for $S = 3/2$ with $g = 2$ in the case of a normal Curie-law system. However, if there is zero-field splitting the magnetization becomes anisotropic, then iso-field curves as a function of temperature do not superimpose. This is due to the differing populations of the components of the zero-field split ground state as the orientation of the magnetic field is varied with respect to the molecule. Consequently, to simulate $M = f(H/T)$ curves it is necessary to evaluate the average of M for all orientations.[20,21] Taking this into account, we have simulated all the magnetization data simultaneously with a full-matrix diagonalization routine using the Hamiltonian (1) with $S = 3/2$ and considering an axial

$$H = D[\hat{S}_z^2 - (1/3)S(S+1)] + g\beta H\hat{S} \qquad (1)$$

crystal zero-field splitting D. The best set of parameters which match the experimental data are found to be $D = 6.2$ cm^{-1}, $g_z = 2.5$ and $g_{x,y} = 2.3$. The solid lines in Figs. 4 and 5 correspond to the calculated curves.

Introducing the calculated D, g_z and $g_{x,y}$ values into the expression (2),[22] which is derived from the Hamiltonian (1), an excellent agreement between the experimental and theoretical $\chi_m T$ data is achieved as observed in Fig. 3. It should be pointed out that the calculated D value could be overestimated because of the possible occurrence of weak intermolecular antiferromagnetic interactions.

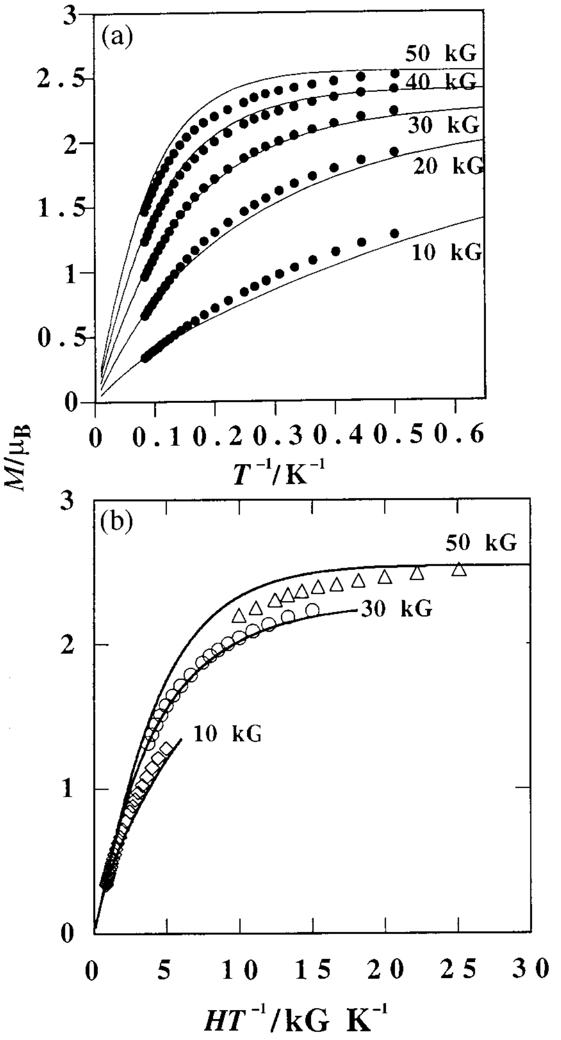

Fig. 5 Magnetization *versus* $1/T$ at various fields (a) and *versus* H/T (b) for complex **1**.

$$\chi_m = \frac{N\beta^2}{3kT}(\chi_z + 2\chi_{x,y}) \tag{2}$$

$$\chi_z = \frac{Ng_z^2\beta^2}{4kT}\,\frac{1 + 9\exp(-2D/kT)}{1 + \exp(-2D/kT)} \tag{3}$$

$$\chi_{x,y} = \frac{Ng_{x,y}^2\beta^2}{kT}\,\frac{1 + (3kT/4D)[1 - \exp(-2D/kT)]}{1 + \exp(-2D/kT)} \tag{4}$$

The idealized geometry of complex **1** belongs to the D_{3h} point group. In this group the orbitals $[d_{yz}, d_{xz}]$, $[d_{x^2-y^2}, d_{xy}]$ and d_{z^2} form the basis for the E″, E′ and A'_1 irreducible representations, respectively. The IS d^5 electronic configuration in D_{3h} has a $^4E''$ orbitally degenerate ground state. Nevertheless, it is apparent that the molecule in this electronic configuration is Jahn–Teller unstable at the regular trigonal bipyramidal geometry. In fact, the actual symmetry of **1** is C_{2v}. In this site symmetry $^4E''$ is split into $^4B_2 + {}^4B_1$ each being further split into Kramers doublets by spin–orbit coupling. If we assume that the distortion with respect to the pure trigonal bipyramid is strong this latter splitting within the quartet states may be smaller than the crystal field splitting. Then $^4B_2$ would be highly stabilized with respect to $^4B_1$ and the orbital degeneracy would vanish (see Scheme 1). The high g_{eff} value of 2.36 observed clearly indicates that the orbital contribution is not completely quenched and that there is some contribution from the $^4B_1$ excited state to the magnetic properties *via* second order spin–orbit coupling.

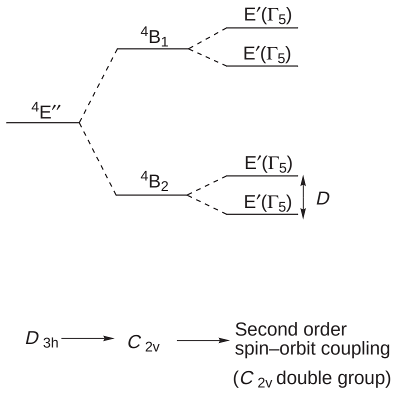

Scheme 1

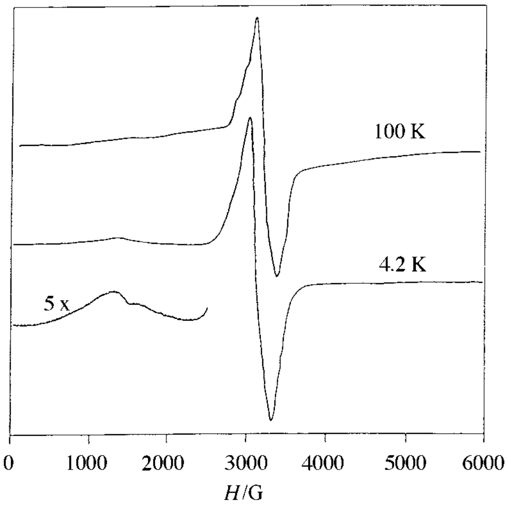

Fig. 6 X-Band EPR spectra of a microcrystalline sample of complex **1**.

EPR Spectra

The X-band EPR spectrum of complex **1** was recorded in the 4.2–300 K range on a polycrystalline sample. It shows a main absorption (see Fig. 6) at 3183 G ($g = 2.13$), for $T = 100$ K. Furthermore, an additional very weak and broad absorption (350 G) is observed at 1440 G ($g = 4.67$), for $T = 4.2$ K. Studies on a dilute frozen glass were precluded given that **1** decomposes in common apolar organic solvents.

Acknowledgements

We are grateful for financial support from the Dirección General de Investigación Científica y Técnica (DGICYT) (Spain) through Project PB94-1002 and the Training and Mobility Research Program from the European Community (TMR Contract ERBFMRXCT-980181). We also acknowledge the Servicio de Difracción de Rayos X de Monocristal de la Universidad Politécnica de Valencia for diffraction facilities.

References

1 J. S. Griffith, *Proc. R. Soc. London, Ser. A*, 1956, **235**, 23.
2 R. L. Martin and A. H. White, *Inorg. Chem.*, 1967, **6**, 712; B. F. Hoskins and A. H. White, *J. Chem. Soc. A*, 1970, 1668.
3 K. L. Kostka, B. G. Fox, M. P. Hendrich, T. J. Collins, C. E. F. Richard, L. J. Wright and E. Munck, *J. Am. Chem. Soc.*, 1993, **115**, 6746.
4 S. Koch, R. H. Holm and R. B. Frankel, *J. Am. Chem. Soc.*, 1975, **97**, 6714.
5 D. H. Dolphin, J. R. Sams and T. B. Tsin, *Inorg. Chem.*, 1977, **16**, 711.
6 D. A. Summerville, I. A. Cohen, K. Hatano and W. R. Scheidt, *Inorg. Chem.*, 1978, **17**, 2906.

7 S. Mitra, V. R. Marathe and R. Birdy, *Chem. Phys. Lett.*, 1983, **17**, 2906.

8 D. Mansuy, I. Morgenstern-Baradau, M. Lange and P. Gans, *Inorg. Chem.*, 1982, **21**, 1427.

9 J. P. Fitzgerald, B. S. Haggerty, A. L. Rheingold, L. May and G. A. Brewer, *Inorg. Chem.*, 1992, **31**, 2006.

10 B. J. Kennedy, K. S. Murray, P. R. Zwack, H. Homborg and W. Kalz, *Inorg. Chem.*, 1986, **25**, 2539.

11 J. S. Griffith, *J. Inorg. Nucl. Chem.*, 1956, **2**, 1.

12 J. S. Griffith, *Discuss. Faraday Soc.*, 1958, **26**, 81.

13 S. M. Nelson, in *Comprehensive Coordination Chemistry*, eds. G. Wilkinson, R. D. Gillard and J. A. McCleverty, Pergamon, Oxford, 1987, vol. 4, p. 217.

14 G. M. Sheldrick, SHELXS 86, A Program for Crystal Structure Determination, University of Göttingen, 1986; SHELXL 93, A Program for the Refinement of Crystal Structures, University of Göttingen, 1993.

15 J. Drummond and J. S. Wood, *Chem. Commun.*, 1969, 1373.

16 J. C. Daran, Y. Jeannin and L. M. Martin, *Inorg. Chem.*, 1980, **19**, 2935.

17 J. A. Real, M. C. Muñoz, E. Andrés, T. Granier and B. Gallois, *Inorg. Chem.*, 1994, **33**, 3587.

18 B. J. Kennedy, G. Brain and K. S. Murray, *Inorg. Chim. Acta*, 1984, **81**, L29.

19 C. A. Reed, T. Mashiko, S. P. Bentlet, M. E. Kostner, W. R. Scheidt, K. Spartalian and G. Lang, *J. Am. Chem. Soc.*, 1971, **101**, 2948.

20 P. D. W. Boyd and R. L. Martin, *J. Chem. Soc.*, *Dalton Trans.*, 1979, 92.

21 M. Gerloch and R. F. McMeeking, *J. Chem. Soc.*, *Dalton Trans.*, 1975, 2443.

22 O. Kahn, *Molecular Magnetism*, VCH, New York, 1993.

Paper 8/09406C